

# Molecular-level understanding of carbon materials by temperature-programmed desorption

Takafumi Ishii\*

International Research and Education Center for Element Science, Faculty of Science and Technology, Gunma University: 1-5-1 Tenjin-cho, Kiryu, Gunma 376-8515, Japan

A wide variety of surface functional groups, such as oxygen-containing ones and hydrogen, exist at the graphene edge sites of carbon materials. Because the presence of these functional groups greatly affects the chemical properties of carbon-based materials produced from them, knowledge of the edge site state is essential to understand carbon chemistry. This review describes the analyses of edge sites and carbon-material structures by temperature-programmed desorption (TPD). Deuterium labeling of the protonic hydrogen of oxygen-containing functional groups enables the precise identification of the chemical structure of edge sites. Furthermore, the spatial distribution of edge sites in the carbon structure can be determined by the kinetic analysis of H<sub>2</sub> desorption spectra collected at temperatures above 1000 °C. The average size of graphene sheets forming the carbon can be estimated from the number of edge sites. The TPD-based analytical approaches described in this paper help provide a better understanding of the carbon structure at the molecular level.

**KEYWORDS :** Carbon edge sites, Temperature programmed desorption, Surface analysis

## 1. Introduction

Carbon consists of crystallites comprising several stacked  $sp^2$  carbon hexagonal networks. The crystallites are divided into basal planes, which form stacking structures via van der Waals forces, and edge sites, which consist of carbon atoms at the edges of the planes. The carbon atoms on the edge sites have unsaturated  $sp^2$  electrons and are chemically more active than those on the basal plane; thus, they can react with different elements, such as oxygen, to form surface functional groups. As shown in **Fig. 1**, a wide variety of surface functional groups, including oxygen-containing functional groups and hydrogen, exist at carbon edge sites. Because the presence of these functional groups significantly affects the chemical properties of carbon surfaces, knowledge of the state (*i.e.*, quality and quantity) of edge sites is essential to understand the chemical properties of carbon.

Various analytical methods are used to determine the state of edge sites. Edge-site analysis is conducted by evaluating and analyzing their characteristics. The characteristics of edge sites can be broadly classified into chemical, optical, electronic, and magnetic properties. **Fig. 2** summarizes the relationships between these characteristics and the major analytical methods for edge sites. Many analytical methods are used to understand edge sites; however, even with these methods,

understanding the nature of edge sites is extremely challenging. The chemistry of carbon materials is often referred to as “black chemistry” because of the difficulty involved in understanding it and the fact that carbon materials are generally colored black [1]. Carbon materials are black because their  $\pi$ -electrons absorb visible light. The  $\pi$ -electrons of  $sp^2$  carbons absorb or shield the analytical probes often used in analytical methods, such as electromagnetic waves and magnetic fields. In addition, the small number of edge sites renders quantitation difficult, leading to problems in analytical precision. Carbon materials are mainly composed of  $sp^2$  carbon and only a very small

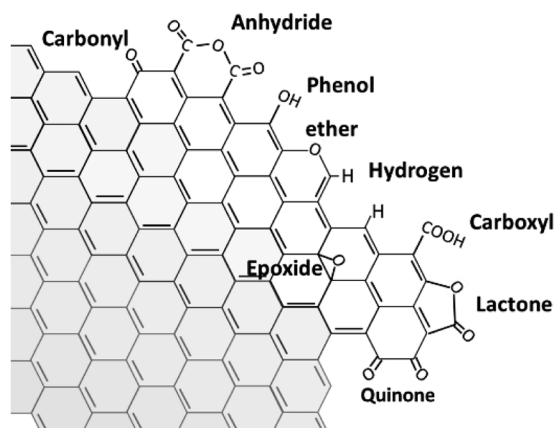


**Fig. 1** Types of functional groups formed at carbon edge sites.

\* Corresponding Author, E-mail: ishii@gunma-u.ac.jp  
<https://doi.org/10.7209/carbon.020203>

(Received February 24, 2023, Accepted March 7, 2023)

proportion (a few atomic percent) of edge sites. High-temperature-treated carbon materials, such as graphite, contain an even smaller percentage of edge sites; for example, surface treatment reduces the percentage of edge sites to approximately  $10^{-4}$  at% [2]. Optimizing the analytical methods and equipment and increasing their sensitivity are challenging but necessary tasks to precisely analyze such a small number of edge sites. In addition to the problem of analytical precision, the author believes that the fact that edge sites are electronically coupled to the massive  $\pi$ -electron system of the carbon network is a major factor hindering the understanding of these sites. Electronic coupling between edge sites and the  $\pi$ -electron system causes not only a shift in the infrared (IR) absorption peak of the functional group formed on them but also the localization and polarization of the  $\pi$ -electrons depending on the edge site state [3], which, in turn, cause the electrons themselves to exhibit magnetism [4, 5] and IR absorption [6]. The unique ability of the  $\pi$ -electron system to take on a variety of states is responsible for the diverse properties of carbon materials, but the existence of these electrons is a major barrier to understanding edge sites.

Temperature-programmed desorption (TPD) is an analytical

method that can probe the desorption reaction of functional groups at edge sites; it is relatively insensitive to the influence of the carbon  $\pi$ -electron system. Here, we use the word “insensitive”, but the influence of the  $\pi$ -electron system on TPD has not been quantitatively clarified. The desorption reaction temperatures of functional groups were previously estimated using quantum chemical calculations with the aid of a small-molecule model that imitated carbon edge sites [7, 8]. Although the calculations were based on a small-molecule model, the results were in good agreement with the desorption reaction temperatures of the same functional groups in actual carbon materials, thus suggesting that the influence of the  $\pi$ -electron system on the corresponding desorption reactions is relatively small. The activation energy for the desorption reaction is strongly affected by the chemical structure of the functional group and, thus, considered to be relatively unaffected by the  $\pi$ -electron system. The shapes of the TPD spectra of activated carbon and graphite (Fig. 3a and b) are very similar, although a large difference in the degree of development of their  $\pi$ -electron systems has been observed. Of course, as shown in Fig. 3, the amount of desorbed gas differs greatly between these materials because their numbers of edge sites completely differ. However, the fact that their

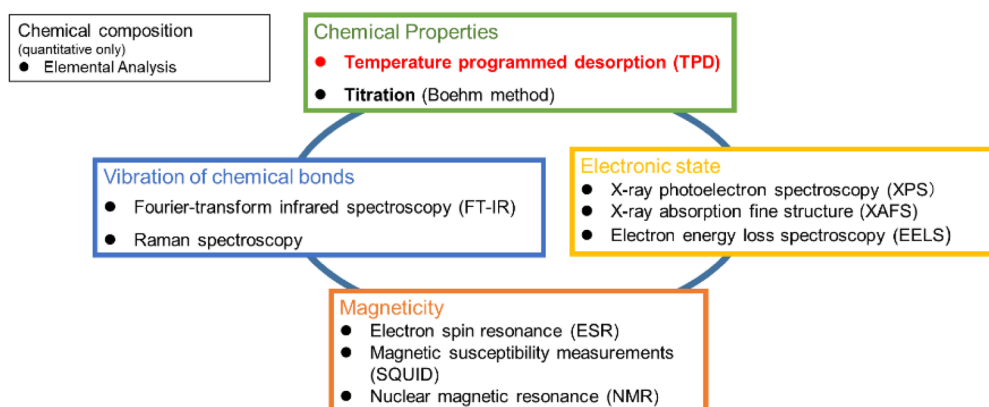


Fig. 2 Analytical methods for carbon edge sites.

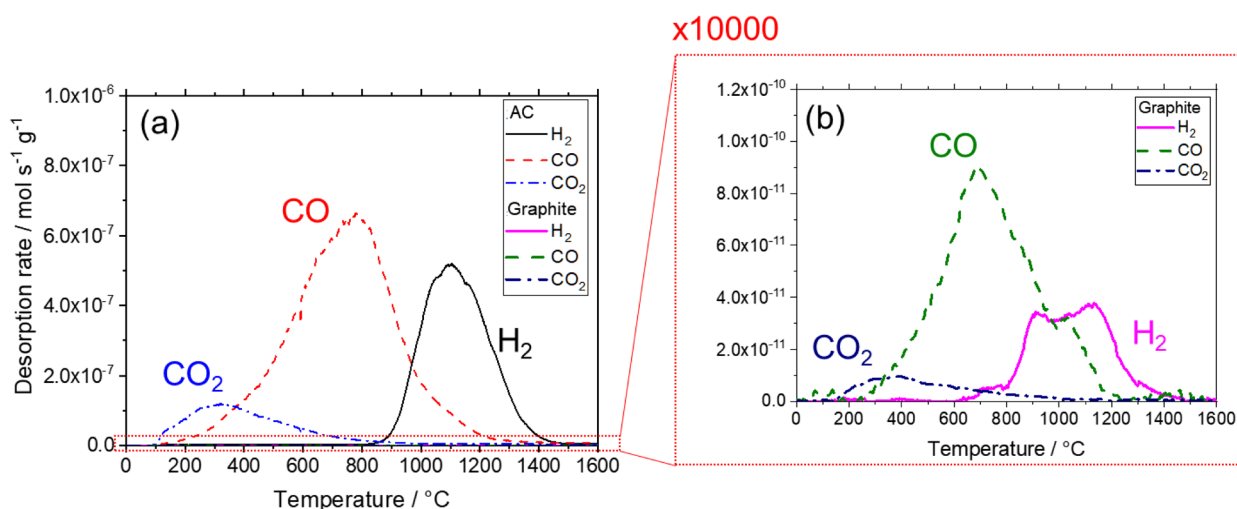


Fig. 3 (a) Comparison of the TPD spectra of activated carbon (MSC30) and natural graphite. (b) Enlarged TPD spectrum of natural graphite.

TPD spectral shapes are very similar indicates, at least experimentally, that the influence of the  $\pi$ -electron system on the TPD spectra is negligible. The author has been developing an analytical method to identify carbon edge sites using TPD. TPD is an analysis method that probes the desorption reaction of functional groups at edge sites. Understanding the chemical process of desorption reaction is essential for its use, but this understanding is not yet sufficient [9]. On the other hand, TPD spectra contain a great deal of information on edge sites, which is important information that cannot be obtained by other analytical methods. This paper introduces the analysis of edge sites, particularly their chemical structure and spatial distribution, using TPD and provides a structural understanding of carbon materials using this method.

## 2. Analysis of Carbon Edge Sites

The edge sites of carbon materials have long been studied in efforts to discuss the chemical properties of carbon. As shown in **Fig. 1**, hydrogen and oxygen-containing functional groups exist at the edge sites of carbon materials, and their qualitative and quantitative determination is extremely important to understand their actual state. Here, the author describes the research related to the qualitative and quantitative determination of hydrogen and oxygen-containing functional groups at edge sites.

Unlike the carbon atoms within crystallites, the carbon atoms at the edge sites of these crystallites have highly reactive and unsaturated bonds that react with different atoms, such as oxygen. Figueiredo *et al.* [10] analyzed the oxygen-containing functional groups on the surface of activated carbon after various oxidation treatments and found that their types varied depending on the oxidation treatment. According to the authors, when activated carbon is subjected to liquid-phase oxidation, oxygen-containing functional groups mainly consisting of carboxyl groups are formed; by contrast, during gas-phase oxidation, oxygen-containing functional groups mainly consisting of carboxylic anhydrides and lactones are formed. Depending on the oxidation conditions, differences in the formation of oxygen-containing functional groups may occur. The oxygen-containing functional groups are described as follows. Oxygen-containing functional groups are broadly classified into acidic, neutral, and basic groups. Acidic functional groups can neutralize bases and are represented by carboxyl and phenolic groups; neutral functional groups include carbonyl groups and ether structures; and basic functional groups can neutralize acids and include chromene-type and pyrone structures [11].

The aforementioned surface oxygen-containing functional groups significantly affect the surface properties of carbon materials, such as their electrochemical properties [12–14], catalytic properties [15], wettability [16] and adsorption characteristics [17]. Many studies have been conducted to analyze the surface oxygen-containing functional groups of carbon materials. These studies are typically accom-

plished using methods such as TPD [18–20], IR spectroscopy [19, 21, 22], X-ray photoelectron spectroscopy (XPS) [23, 24], and Boehm titration [25, 26]. However, even with these methods, determining the chemical forms of complex functional groups on carbon is difficult. IR spectroscopy provides information on the chemical bonds of functional groups, whereas XPS provides information on their charge distributions. A common feature of these two analytical methods is that they provide local information on chemical structures. Thus, they cannot distinguish between ethers (C–O–C), lactones, and acid anhydrides. Boehm titration provides information on acidic functional groups but not on neutral functional groups, such as carbonyl groups. The acid strength of acidic functional groups does not directly represent their chemical form; thus, determining the chemical form of these groups using Boehm titration is difficult. Furthermore, edge sites are present in the carbon structure at only trace amounts, ranging from approximately 1 at% in activated carbon to less than 0.01 at% in graphite. Given the difficulty of evaluating such trace amounts using the existing analytical methods and the complexity of edge sites, their chemistry remains largely unknown.

In addition to oxygen-containing functional groups, hydrogen is present at edge sites. Because carbon is formed by the carbonization of organic materials, hydrogen atoms are present in carbon. Most edge sites in carbon materials that are not oxidized or treated otherwise are terminated by hydrogen. **Fig. 4a** summarizes the changes in the numbers of hydrogen and oxygen-containing functional groups in various carbon materials as a function of the heat-treatment temperature. The hydrogen content was approximately 1–100 times larger than the oxygen-containing functional group content, and the difference between these contents decreased as the heat-treatment temperature increased. In particular, at heat-treatment temperatures below 1800 °C, over 90% of the edge sites were terminated with hydrogen, which is the main functional group constituting the carbon edge site. The hydrogen and oxygen contents of various carbon materials are summarized in **Fig. 4b**. Although the nature and quantity of the edge sites varies greatly depending on the type of carbon material and heat treatment temperature, the hydrogen content is higher than the oxygen content in most of the materials. Although the amount of hydrogen in carbon is important for obtaining information on edge sites, quantitative analysis is difficult because the weight fraction of hydrogen is small, the error due to the effect of adsorbed water is large, and hydrogen analysis is spectroscopically difficult. Kashihara *et al.* [27] successfully determined the hydrogen content of graphitizable and non-graphitizable carbons heat-treated at 1000–1800 °C by temperature-programmed oxidation using a Karl Fischer moisture analyzer. The authors found that the hydrogen content of carbon was independent of its structure and depended only on the heat-treatment temperature; they also reported that the hydrogen content of high-temperature-treated carbon was extremely low, ranging from 0.002 to

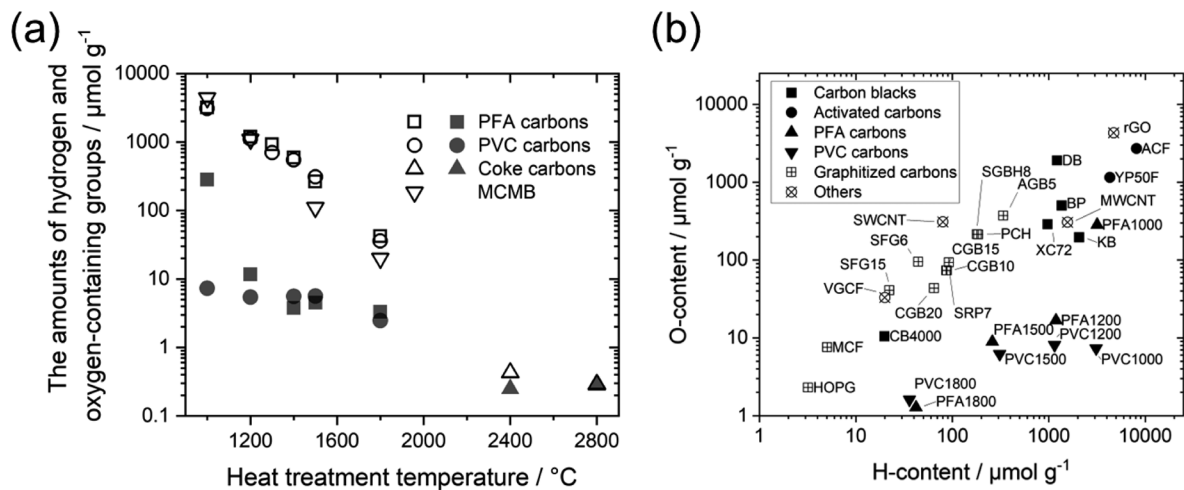


**Fig. 4** (a) Variation in the contents of hydrogen and oxygen-containing functional groups of carbon materials as a function of the heat-treatment temperature. Reproduced with permission from ref. 2. Copyright 2022 Elsevier. (b) Relationship between hydrogen and oxygen contents for various carbon materials [48, 67]. The numbers at the end of PFA and PVC carbons indicate the heat treatment temperature ( $^{\circ}\text{C}$ ).

0.007 wt%, after heat treatment at 1800  $^{\circ}\text{C}$ . Determination of the hydrogen content of high-temperature-treated carbon is extremely difficult; indeed, to the author's best knowledge, only Meyer *et al.* [28] has successfully measured hydrogen contents by burning three types of carbon that had been heat-treated at 800–2900  $^{\circ}\text{C}$ . The authors reported that the hydrogen content of carbon heat-treated at 800  $^{\circ}\text{C}$  was approximately 0.14 wt% and decreased to 0.015–0.002 wt% when the heat-treatment temperature exceeded 2000  $^{\circ}\text{C}$ .

### 3. Temperature-programmed Desorption

#### 3.1 Analysis of oxygen-containing functional groups

TPD (also called thermal desorption spectrometry) was originally developed as a method to analyze the adsorbed gases in a sample, particularly in the field of catalytic chemistry. It is now widely used to analyze not only adsorbed materials but also the surface and near-surface conditions of various materials. During TPD, the gases generated by the desorption of surface functional groups are qualitatively and quantitatively analyzed by heating carbon in an inert atmosphere or vacuum. The quality and quantity of surface functional groups can be determined from the TPD spectrum, in which the horizontal axis is the temperature and the vertical axis is the desorption rate. TPD has been used to analyze many carbon materials since the relationship between oxygen-containing functional groups on the surface of carbon and their desorption temperatures was first reported in 1978 [29]. The reported values for the types of carbon materials and their oxygen-containing functional groups are summarized in Fig. 5 [2, 30–48]. TPD analysis has also been recently applied to nanocarbon materials, such as reduced graphene oxide and carbon nanotubes (CNTs; *e.g.*, single- and multiwalled CNTs). The oxygen-containing functional groups of porous carbon materials such as activated carbon range from several hundred to several thousand micromoles per gram, with

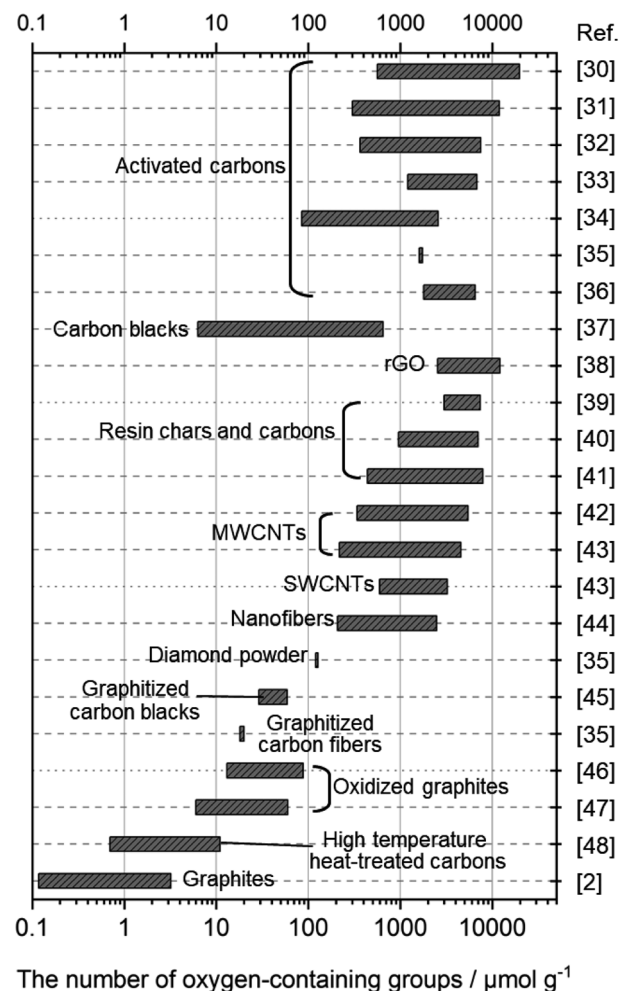


**Fig. 5** Numbers of oxygen-containing functional groups in various carbon materials.

some even exceeding 10,000  $\mu\text{mol g}^{-1}$ . By contrast, the oxygen-containing functional group content of high-temperature-treated carbon is less than 100  $\mu\text{mol g}^{-1}$ , while that of graphite is even less (less

than a few micromoles per gram). One of the advantages of TPD as an analytical method is that it is applicable to materials with widely varying numbers of functional groups.

Surface oxygen-containing functional groups produce CO, CO<sub>2</sub>, and H<sub>2</sub>O upon desorption, and the structure and amount of each functional group can be estimated by analyzing the gases desorbed during the TPD measurements. **Table 1** summarizes the previously reported surface oxygen-containing functional groups, desorption temperatures, and desorbed gases. Most oxygen-containing functional groups were desorbed at temperatures below 1000 °C, and the desorption temperatures varied, even for the same types of oxygen-containing functional groups. The desorption temperature of oxygen-containing functional groups is affected by many factors, such as the heating rate and apparatus configuration [10]. Furthermore, the chemical structure of edge sites around these groups affects their desorption temperature. For example, if two carboxyl groups are adjacent to each other, their desorption temperatures will be lower than that of a single carboxyl group [7]. Thus, the results obtained from TPD measurements contain a great deal of information about edge sites and contribute greatly to

the essential understanding of the chemical structures of these sites. However, TPD spectra are affected by many factors, such as secondary reactions and impurity effects [49], and their interpretation is challenging and remains a subject of debate. Thus, further research is warranted.

### 3.2 Accurate analysis of the chemical structure of edge sites

As mentioned above, TPD enables the qualitative analysis of functional groups based on differences in their desorption reaction behavior (*i.e.*, desorption temperature and gas). The desorption reaction of a functional group strongly depends on its chemical form, and both the desorption temperature and gas differ depending on the functional group. For example, ether, lactone, and anhydride are known to desorb as CO, CO<sub>2</sub>, and CO+CO<sub>2</sub>, respectively, and their functional groups can be distinguished by the differences in these desorption gases. However, some functional groups, including phenol (C–OH) and ether (C–O–C), cannot be identified by TPD analysis. These functional groups are known to desorb as CO at approximately 600–700 °C; therefore, they are indistinguishable by TPD analysis

**Table 1** Types of oxygen-containing functional groups, their desorption gases, and desorption temperatures.

Desorption gas	Temperature/°C	Atmosphere	Desorption gas	Temperature/°C	Atmosphere
Phenol			Carboxylic		
CO	617–637 [10]	He	CO <sub>2</sub>	100–400 [10]	He
	600–700 [50]	Ar		200–250 [50]	Ar
	550 [51]	He		250 [18]	N <sub>2</sub>
	627–657 [52]	Vac.		250–300 [51]	He
Carbonyl and Quinone				100–400 [53]	He
CO	787–827 [10]	He		247–287 [52]	Vacuum
	800–900 [50]	Ar		302 [53]	He
	700–980 [54]	Vacuum		277 [55]	He
	702, 835 [55]	He		CO+H <sub>2</sub> O	242, 327 [56]
	700–980 [57]	Vacuum	Lactone		
Ether			CO <sub>2</sub>	667 [10]	He
CO	827 [10]	He		350–400 [50]	Ar
	550 [51]	He		450 [51]	He
Aldehyde				190–650 [54]	Vacuum
CO	280 [58]	He		519 [55]	He
	310 [59]	He		150–650 [57]	Vacuum
Acid anhydride				627 [20]	He
CO+CO <sub>2</sub>	547 [10]	He	Peroxide		
	350–400 [50]	Ar	CO <sub>2</sub>	550–600 [50]	Ar
	627 [18, 20]	N <sub>2</sub>		597 [52]	Vacuum
	407–447 [52]	Vacuum	Phosphorus (C–O–POx)		
	427–502 [53]	He	CO	800 [60]	N <sub>2</sub>
	437–657 [55]	He		860 [61]	N <sub>2</sub>



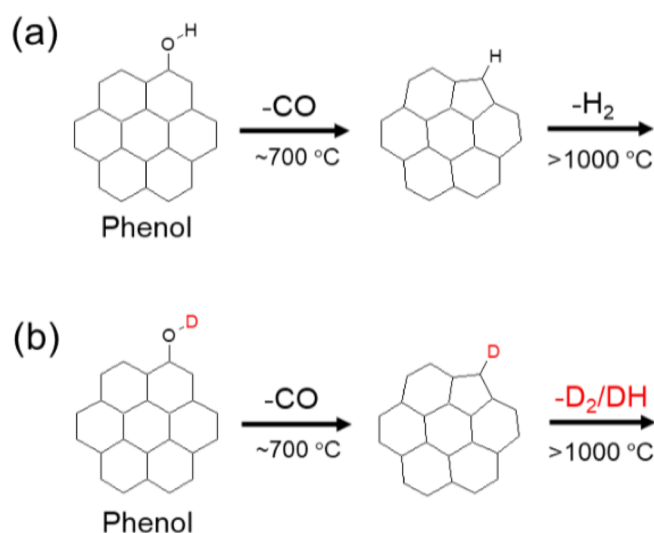


**Fig. 6** Desorption behavior of (a) phenolic group and (b) deuterium-labeled phenolic group on the surface of carbon materials. Reproduced with permission from ref. 63. Copyright 2019 Elsevier.

because their desorption temperatures and gases are identical.

During TPD analysis, the desorption behaviors of phenol and ether do not completely coincide because phenol contains hydrogen in its chemical structure, as shown in **Fig. 6**, and the hydrogen is desorbed as  $\text{H}_2$  with further increases in temperature. Because  $\text{H}_2$  desorption requires a temperature of over  $1000\text{ }^\circ\text{C}$ , it has not been evaluated or discussed via TPD owing to analytical difficulties. The authors reported the analysis of hydrogen-terminated edge sites (edge hydrogens) via TPD at temperatures of over  $1600\text{ }^\circ\text{C}$  [2, 48, 62]. At such high temperatures, edge hydrogen is desorbed as  $\text{H}_2$ , and the amount of edge hydrogen can be estimated by quantification (see Section 3.3). The temperature limit for conventional TPD is about  $1100\text{ }^\circ\text{C}$ , and it is not possible to detect the desorption of  $\text{H}_2$ . TPD analysis at high temperatures can detect the desorption of  $\text{CO}$  and  $\text{H}_2$ , which may allow us to distinguish between phenol and ether. However, one issue that must be considered here is that the  $\text{H}_2$  desorbed at high temperatures includes not only phenol-derived  $\text{H}_2$  but also edge hydrogen-derived  $\text{H}_2$ , and distinguishing between these gases is impossible. The hydrogen in phenol is protonated; therefore, it can easily be replaced by deuterium in the presence of  $\text{D}_2\text{O}$ . In a previous study, activated carbons with deuterium-labeled oxygen-containing functional groups were prepared, and TPD was performed to analyze the chemical structure of the carbon edge sites in detail [63]. The TPD spectra of activated carbons labeled with deuterium by immersion in  $\text{D}_2\text{O}$  are shown in **Fig. 7**; here, a total of eight spectra indicating deuterium compounds,  $\text{H}_2$ ,  $\text{CO}$ , and  $\text{CO}_2$  desorption species are obtained. This large collection of spectra is advantageous because it provides a great deal of information on oxygen-containing functional groups. However, their interpretation is rather complex. To identify the oxygen-containing functional groups from these TPD spectra, we must

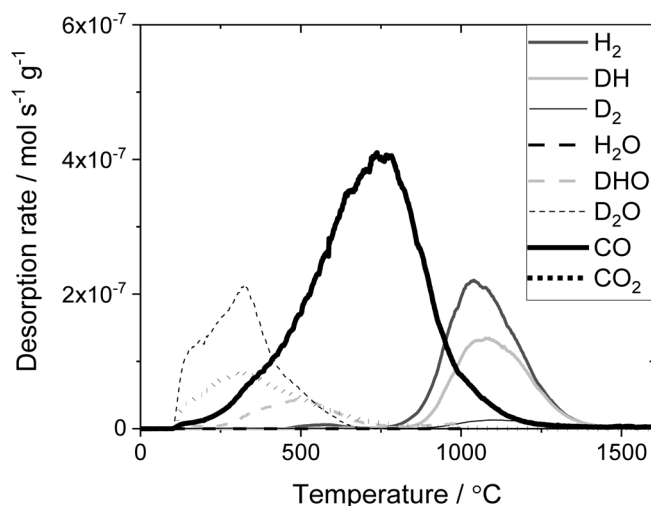


**Fig. 7** TPD spectra of deuterium-labeled activated carbon (MSC30).

first consider the desorption mechanism of deuterium compounds. **Fig. 8a** summarizes the desorption mechanism of each deuterium compound. The chemical structures shown are distinguishable because they follow different desorption processes. For example, three chemical structures were desorbed as  $\text{D}_2\text{O}$ :  $\text{C}_x\text{C}_2$ ,  $\text{C}_x\text{Ph}$ , and  $\text{Ph}_2$ .  $\text{C}_x\text{C}_2$  forms  $\text{D}_2\text{O}$ , which then forms an anhydride and is desorbed as  $\text{CO} + \text{CO}_2$  upon further heating. Similarly,  $\text{C}_x\text{Ph}$  forms a lactone and  $\text{Ph}_2$  forms an ether; therefore, although their  $\text{D}_2\text{O}$  formation processes are similar, the chemical structures of these three species can be distinguished because the subsequent desorbed gases are different. Thus, the chemical structures of edge sites can be classified into 12 types, as shown in **Fig. 8b**, according to their higher-order chemical structures, including the surrounding parts of the functional groups. **Table 2** summarizes the relationships between these 12 chemical structures and the desorbed gas species. The quantitative results of the edge-site chemical structures of the deuterium-labeled samples are shown in **Fig. 8c**. Phenols and ethers can be quantitatively distinguished, and even the same functional groups can be distinguished based on differences in the chemical structure around the functional group. Furthermore, because the analytical principle of TPD is the distinction between protic and edge hydrogens, both oxygen-containing functional groups and edge hydrogens can be accurately quantified. The IR spectra of the samples were estimated using DFT calculations based on this quantitative result, and the calculated IR spectra agreed well with the experimental values (**Fig. 8d**). Thus, deuterium labeling can dramatically improve the accuracy of the TPD method and, in turn, lead to a deeper understanding of the chemical structure of carbon edge sites.

### 3.3 Evaluation of the spatial distribution of edge sites

Although edge hydrogen is thermally stable, it can be analyzed via TPD by heating up to approximately  $1600\text{ }^\circ\text{C}$ . **Fig. 9** shows the TPD spectrum of activated carbon (YP50F); here, the  $\text{H}_2$  desorption peak can be observed in the range of  $800\text{--}1500\text{ }^\circ\text{C}$ . The  $\text{H}_2$  desorp-

**Table 2** Relationships between desorbed species determined by TPD measurement and chemical species formed on carbon edge sites. The label in parenthesis indicates the gas species divided into its source functional groups as a result of peak separation of TPD spectra.

Desorbed species	Chemical species
D (from D <sub>2</sub> and DH)	Ph1+Cx1
D <sub>2</sub> O	Cx2+CxPh+Ph2
DHO	PhH+CxH
CO <sub>2</sub> (Carboxylic)	Cx1
CO <sub>2</sub> (Lactone)	CxPh+Lactone
CO (Anhydride)	Cx2+Anhydride
CO (Phenol/Ether)	Ph1+Ph2+Ether
CO (Carbonyl)	Carbonyl+CxH
H (from H <sub>2</sub> and DH)	Edge H

tion amount obtained from TPD was consistent with that obtained using the combustion method, indicating that most of the edge hydrogen contained in the sample is desorbed when the temperature is increased up to 1600 °C.

In recent years, the quantitative analysis of edge hydrogen has become increasingly important for understanding the chemical reactivity of carbon materials. As discussed in literatures [37, 64–66], earlier studies have demonstrated that edge hydrogen behaves as an active site in carbon surface chemistry. As mentioned above, the quantitative analysis of edge hydrogen by high-temperature TPD is now possible. However, the qualitative meaning of the H<sub>2</sub> desorption spectra has not been elucidated although the TPD spectra are inherently interpreted in terms of the kinetics of the desorption reaction, and the peak

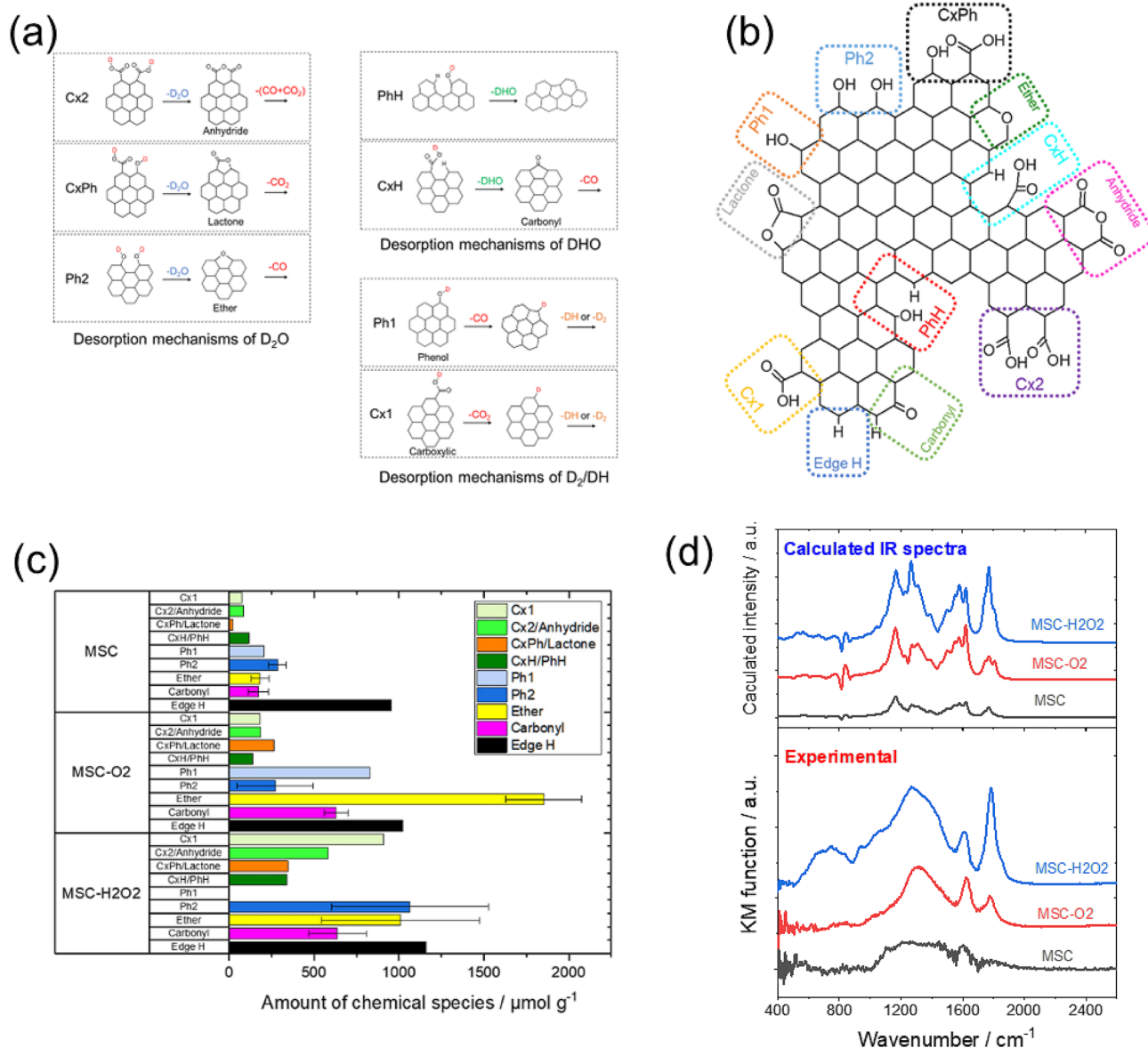


**Fig. 8** (a) Desorption mechanism of deuterium compounds. (b) Twelve types of edge-site chemical structures distinguishable by deuterium-labeled TPD. (c) Quantification of the edge-site chemical structures of activated carbon samples. The samples included activated carbon (MSC), O<sub>2</sub>-oxidized activated carbon (MSC-O2), and H<sub>2</sub>O<sub>2</sub>-oxidized activated carbon (MSC-H2O2). (d) Calculated (top) and experimental (bottom) IR spectra of the samples. Reproduced with permission from ref. 63. Copyright 2019 Elsevier.

temperatures and shapes should contain qualitative information about the desorbed species. The author performed a kinetic analysis of the H<sub>2</sub> desorption spectra collected in TPD measurements [67]. Arrhenius analysis of these spectra indicated that the H<sub>2</sub> desorption reaction was caused by the association of edge hydrogens and that the reaction order was 2. Furthermore, the apparent activation energy for the H<sub>2</sub> desorption reaction estimated by Arrhenius analysis was consistent

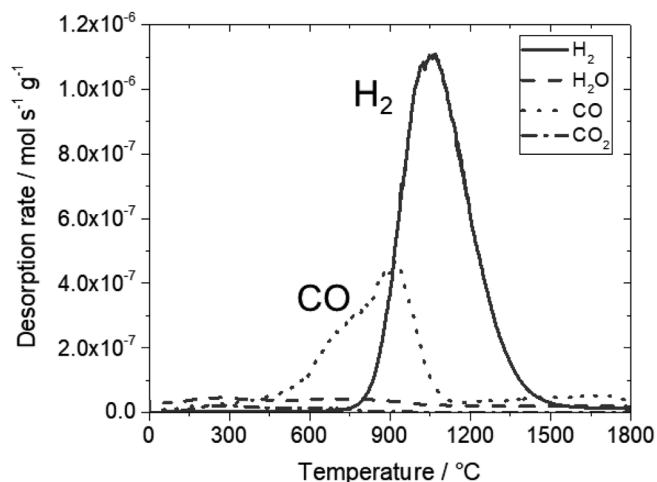


Fig. 9 TPD spectra of activated carbon (YP50F).

with that of the edge-hydrogen association reaction estimated by density functional theory calculations. The H<sub>2</sub> desorption reaction rate  $D_{H_2}(T)$  observed via TPD at absolute temperature  $T$  was determined using the Polanyi–Wigner equation [68] by considering the concentration of edge hydrogen in the carbon sample at this temperature  $A_H(T)$  as follows:

$$D_{H_2}(T) = -\frac{1}{2} \cdot \frac{dA_H(T)}{dT} = \frac{1}{2} \cdot \frac{\nu}{\beta} (\alpha_H A_H(T))^2 \exp\left(\frac{-E_d}{RT}\right), \quad \dots (1)$$

where  $\nu$  is the frequency factor,  $\beta$  is the heating rate,  $\alpha_H$  is the activity coefficient,  $E_d$  is the activation energy of the desorption reaction, and  $R$  is the gas constant. To calculate  $A_H(T)$ , we assume that the edge hydrogen is uniformly distributed in the sample, and that the concentration of the edge hydrogen at 1600 °C (the maximum TPD temperature) is zero. Under these assumptions,  $A_H(T)$  can be calculated using the following equation:

$$A_H(T) = 2 \int_T^{1873.15} D_{H_2}(T) dT. \quad \dots (2)$$

At the peak temperature  $T_P$  of the H<sub>2</sub> desorption spectrum, the following equation is satisfied:

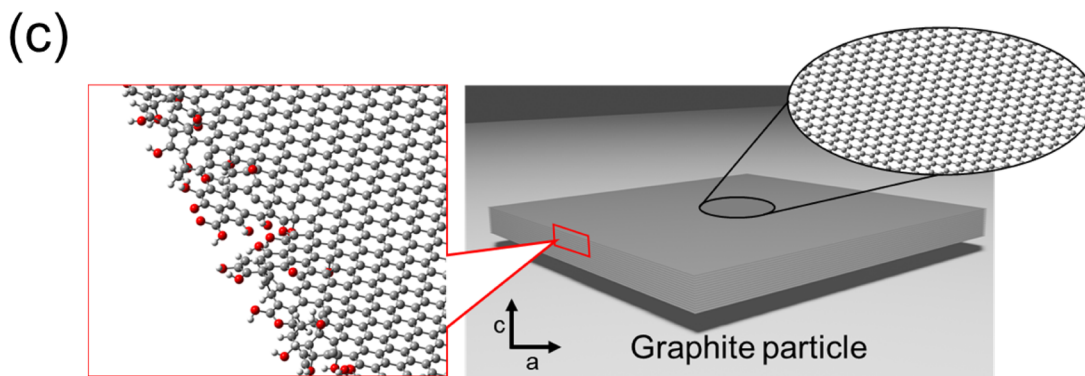
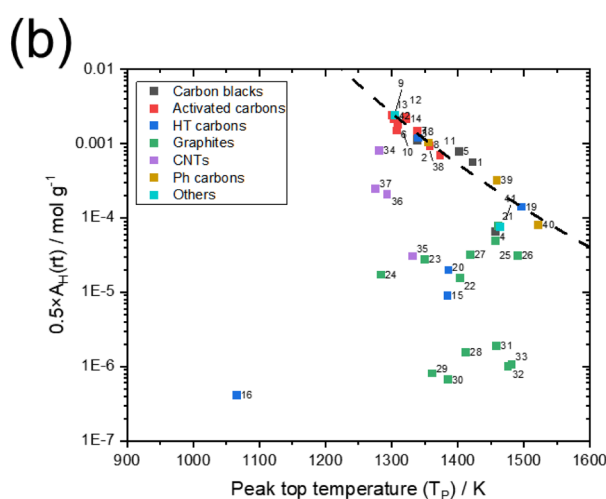
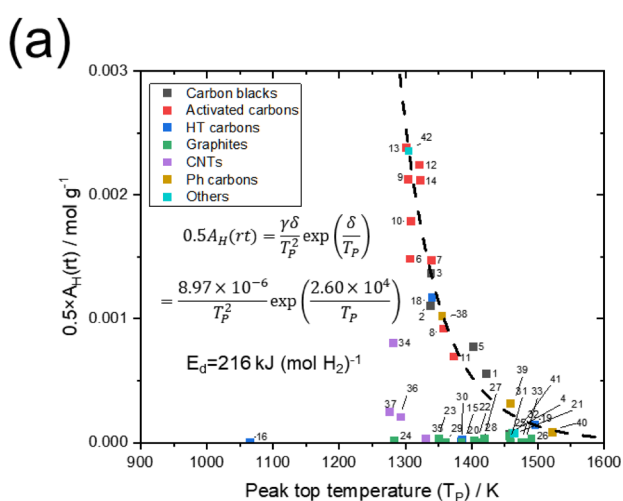


Fig. 10 (a, b) Relationship between the peak temperature ( $T_P$ ) and concentration of edge hydrogen  $A_H(rt)$ . The points in each plot indicate the sample number in the reference. The black dashed lines indicate the relationship in Equation (6). (c) Spatial distribution of edge sites in graphite particles demonstrated in our previous study. Reproduced with permission from ref. 2. Copyright 2022 Elsevier.



$$\frac{d^2 A_H(T_P)}{dT^2} = 0. \quad \dots\dots\dots (3)$$

From the above equations, the concentration of edge hydrogens at temperature  $T_P$ ,  $A_H(T_P)$ , can be expressed using  $T_P$  as follows:

$$A_H(T_P) = \frac{\beta E_d}{2\alpha_H^2 \nu R} \cdot \frac{1}{T_P^2} \exp\left(\frac{E_d}{RT_P}\right). \quad \dots\dots\dots (4)$$

When fitting the hydrogen desorption spectrum with a Gaussian function,  $A_H(T_P)$  can be expressed as follows by assuming that all edge hydrogens are desorbed in the TPD run.

$$A_H(T_P) = \frac{1}{2} A_H(\text{rt}). \quad \dots\dots\dots (5)$$

where  $A_H(\text{rt})$  is the concentration of the edge hydrogen at room temperature. Give this relation, Equation (4) becomes synonymous with the following equation:

$$\frac{1}{2} A_H(\text{rt}) = \frac{\beta E_d}{2\alpha_H^2 \nu R} \cdot \frac{1}{T_P^2} \exp\left(\frac{E_d}{RT_P}\right). \quad \dots\dots\dots (6)$$

A plot of  $A_H(\text{rt})$  versus  $T_P$  for a wide variety of carbon samples is shown in **Fig. 10**. The  $T_P$  values of these samples were obtained by fitting the  $H_2$  desorption spectra with a Gaussian function. Because  $A_H(T)$  (including  $A_H(\text{rt})$ ) is calculated under the assumption that the edge hydrogen is uniformly distributed in the structure of the carbon sample (Equation (2)),  $A_H(\text{rt})$  and  $T_P$  must satisfy the relationship shown in Equation (6) (this relationship is also reflected by the dashed line in the figure). A carbon sample falling outside the dashed line indicates that the edge hydrogen atoms are nonuniformly distributed in the carbon structure. For commercially available activated carbon, carbon black, and carbon obtained by heat treatment below  $1200^\circ\text{C}$ , the relationship between  $A_H(\text{rt})$  and  $T_P$  is satisfactory. However, this relationship does not apply to high-temperature-treated carbon, graphite, and CNTs, indicating that the edge hydrogens are nonuniformly distributed in the structure of these carbon samples. In our previous study, we analyzed the molecular structures of high-temperature heat-treated carbons, such as graphite, using accurate analytical techniques [2]. In this study, we demonstrated that natural graphite particles contain edge sites only on their surface; such sites are not found within the particles. Additionally, the surrounding region of the particles exhibited complex disorder at the molecular level, with a large number of edge sites, as shown in **Fig. 10c** (details are provided in Section 4). This result implies that the edge sites of graphite are distributed locally within a portion of its carbon structure. This property of graphite is related to the fact that almost all graphite samples deviate from the relationship between  $A_H(\text{rt})$  and  $T_P$ . Similar to graphite, CNTs and high-temperature-treated carbons also deviate from this relationship, thereby implying that these samples may also contain locally distributed edge hydrogens in their carbon

structures. The  $H_2$  desorption spectra obtained by high-temperature TPD include information on not only the amount of edge hydrogens but also their spatial distribution in a carbon structure. Such information cannot be obtained by other techniques such as elemental analysis, thus suggesting that TPD is an extremely powerful, irreplaceable tool for edge-site analysis.

#### 4. Determination of Carbon Structure from the Amount of Edge Sites

Aso *et al.* [69, 70] applied the elemental composition method to analyze the organic structure of carbon materials heat-treated below  $1000^\circ\text{C}$  and determined the average size of a graphene sheet (**Fig. 11a**),  $L$ , from the number of edge sites [70]. This size was reported to be larger than that obtained from XRD analysis ( $L_a$ ) and TEM observations ( $L_{\text{TEM}}$ ). As illustrated in **Fig. 11b**, the difference in graphene size can be attributed to the fact that XRD and TEM cannot accurately measure the length of a curved graphene sheet.

This structural analysis of carbon based on the number of edge sites is also useful for investigating high-temperature-treated carbons. The same analysis was performed on non-graphitizable and graphitizable carbons treated at high temperatures ( $1200\text{--}1800^\circ\text{C}$ ); here, the structure of non-graphitizable carbon was found to be formed by the extremely complex bending of large graphene sheets. Furthermore, the sheet sizes of high-temperature-treated carbons depended only on the heat-treatment temperature, regardless of the type of carbon (non-graphitizable or graphitizable) [48]. **Table 3** summarizes the results of the determination of edge sites and values of  $L$ ,  $L_{\text{TEM}}$ , and  $L_a$

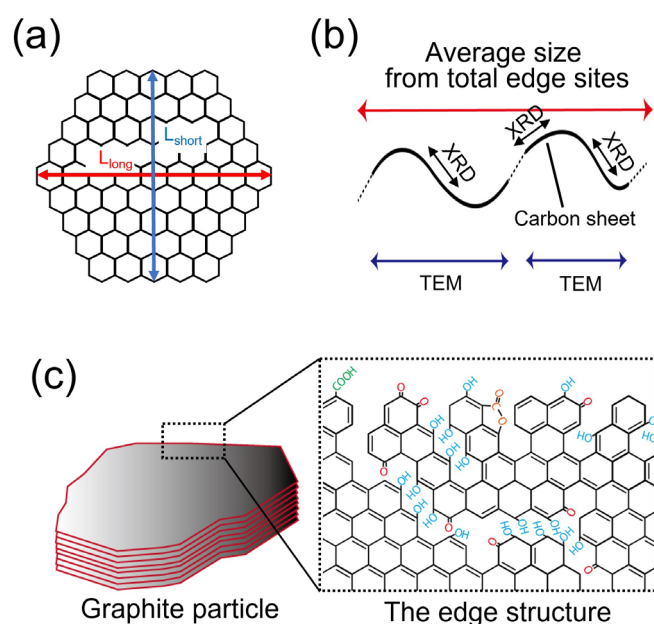


**Fig. 11** (a) Structural model of a graphene sheet. (b) Conceptual image of the process of obtaining the graphene sheet size from the number of edge sites. (c) Chemical structure of edge sites formed in a graphite particle. Reproduced with permission from ref. 70. Copyright 2004 Elsevier.

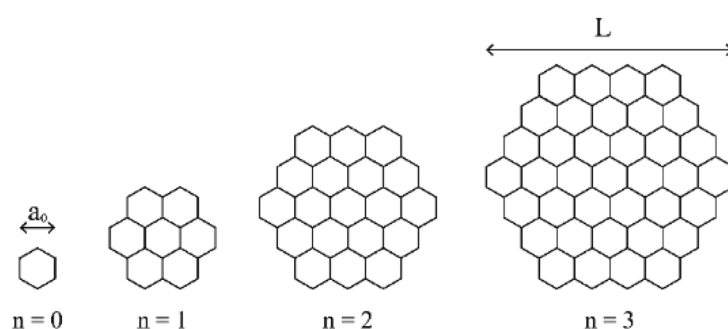
for the carbons in heat-treated polyfurfuryl alcohol (PFA) and polyvinyl chloride (PVC), where  $L$  is calculated using the coronene-based models shown in Fig. 12. The values of  $L$  depend only on the heat-treatment temperature, regardless of the structures of the PFA and PVC carbons, although these are completely different.  $L$  calculated from the number of edge sites was consistently larger than  $L_{\text{TEM}}$  and  $L_a$  for both samples. This finding may be attributed to the fact that  $L$  reflects the entire graphene sheet, whereas  $L_a$  refers only to the size of the crystallites and  $L_{\text{TEM}}$  is the result of a two-dimensional analysis of the cross-section of the graphene sheet; hence,  $L_a$  and  $L_{\text{TEM}}$  do not reflect the entire three-dimensional curved graphene sheets. According to XRD and TEM observations, the structure of PFA carbon is considered to be a disorderly arrangement of small graphene sheets of approximately 5 nm; however, these small graphene sheets are connected to each other and may be expected to form a complex curved large graphene sheet.

The advantage of structural analysis using the number of edge sites

is that it can determine the average size of a complex aligned and curved graphene sheet. Thus, it may be a powerful tool for understanding the actual carbon structure. This technique can be applied to graphite to obtain an actual picture of edge sites that are disordered at the molecular level (Fig. 11c) [2]. Two types of graphite samples (NG50 and NG160) with different particle sizes were prepared by fractionating natural graphite powder (Alfa Aesar; purity, 99.9995%). These graphite samples were heat-treated under vacuum at 1800 °C for 1 h for surface cleaning and denoted as NG50HT and NG160HT, respectively. The numbers of edge sites in these samples were much smaller than those in PFA and PVC carbons, as shown in Table 3. Furthermore, the numbers of edge sites in the graphite samples decreased significantly with heat treatment. The  $L$  of the heat-treated graphite samples was extremely large, and, surprisingly, its value was almost equal to their particle size. This finding indicates that the edge sites exist only around the particles. The structure of the graphite sample obtained after heat treatment is understood to consist of

**Table 3** Amounts of total edge sites and sizes of the carbon layer ( $L$ ) calculated using the coronene-based model for different carbon samples and crystallite sizes determined by the image processing of the TEM images and X-ray diffractograms.

Sample	Total edge sites / $\mu\text{mol g}^{-1}$	$L/\text{nm}$	$L_{\text{TEM}}/\text{nm}$	$L_a/\text{nm}$
PFA1200	1240–1400	30–33	5.1	3.6
PFA1500	260–390	105–158	5.2	4.2
PFA1800	41–95	430–1000	5.5	4.2
PVC1200	1130–1250	33–35	27	4.2
PVC1500	310–340	121–132	42	6.8
PVC1800	35–37	720–1170	60	8.4
NG50	6.5	6300	O.L.	320
NG150	5.3	7800	O.L.	670
NG50HT	0.62–0.74	55000–66000	O.L.	370
NG150HT	0.15–0.20	207000–271000	O.L.	650



$$N_{\text{edge}} = \text{free sites} + H + \text{carbonyl} + \text{ether} + 2 \cdot \text{anhydride} + 2 \cdot \text{lactone}$$

$$L = a_0(2n + 1) \cong \frac{2Ca_0}{N_{\text{edge}}} \quad (C \gg \text{other species})$$

**Fig. 12** Coronene-based models used to calculate the size of a graphene sheet ( $L$ ) and the corresponding equations used to calculate  $L$  from the numbers of edge sites. In the equations,  $N_{\text{edge}}$ ,  $a_0$ , *free sites*, *H*, *C*, *ether*, *carbonyl*, *anhydride*, and *lactone* correspond to the total number of edge sites, lattice parameter of the *a*-axis (0.2461 nm), and numbers of free sites, hydrogen atoms, carbon atoms, ether, carbonyl, acid anhydride, and lactone groups per unit weight of each carbon sample, respectively. The free sites represent the edge site of the triplet carbene/carbyne and the doublet  $\sigma$ -radical sites, and its amount was calculated from the amount of electron spin determined by magnetic susceptibility measurements. Reproduced with permission from ref. 48. Copyright 2014 Elsevier.

stacked graphene sheets equivalent in size to the graphite particles. As imagining that such an extremely large graphene sheet could be generated by heat treatment at 1800 °C is difficult, we can reasonably assume that the graphite sample had a similar carbon structure before heat treatment. In other words, the edge sites of the graphite sample before heat treatment were located around its particles, where a large number of edge sites exist, as shown in **Fig. 10c**. This finding indicates that the edge sites of graphite are locally distributed in one part of its carbon structure. Such a distribution is consistent with the aforementioned kinetic analysis of the hydrogen desorption spectrum. Although a definitive answer to how the edge sites of graphite are formed has not yet been obtained, they are believed to be formed by pulverization and other processes during manufacturing.

The same type of analysis has recently been used to evaluate the structure of extremely complex materials such as graphene oxide [71], and the applicability of this method is expected to expand. The precise analysis of edge sites and their application to the structural analysis of carbon materials can be used to obtain a detailed understanding of the actual carbon structure and appearance of edge sites, which cannot be achieved by other types of analyses.

## 5. Conclusion

This review describes the analysis of carbon edge sites via TPD and discusses carbon structures in terms of the number of edge sites. Oxygen-containing functional groups and hydrogen atoms exist at carbon edge sites, and their nature and quantity vary depending on the carbon material. Furthermore, the average carbon structure can be predicted from the number of edge sites obtained by TPD to gain a deeper understanding of the carbon structure. Edge sites provide information on not only the chemical properties of carbon materials but also their structural characteristics. However, TPD cannot always identify functional groups. To solve this problem, we introduced the deuterium-labeled TPD method, in which protonic hydrogen is labeled with deuterium. The spatial distribution of edge sites can be determined by evaluating the hydrogen desorption spectra collected during TPD. By combining these experimental and analytical methods, TPD may be expected to be of great help in understanding the molecular structures of carbon materials. The TPD spectrum is a two-dimensional representation of the relationship between the desorption temperature and rate of a desorbed gas, which initially seems simple. However, the essence of TPD is the desorption reaction, which involves the chemistry of carbon surfaces. Obtaining a deeper understanding of TPD will allow us to obtain more accurate insights into the essence of carbon surfaces. Although TPD is not fully understood even in the field of carbon materials, future improvements and innovations in analytical techniques could lead to remarkable advancements in our understanding of TPD.

## Acknowledgements

The author is grateful to Prof. Takashi Kyotani and Prof. Junichi Ozaki for their supervision during this study.

## References

- [1] J. Ozaki, *カーボンアロイ触媒と燃料電池* [title in Japanese], Kagaku to kyoiku 59 (2011) 254–257 [in Japanese].
- [2] T. Ishii, Y. Kaburagi, A. Yoshida, Y. Hishiyama, H. Oka, N. Setoyama, J. Ozaki, T. Kyotani, Analyses of trace amounts of edge sites in natural graphite, synthetic graphite and high-temperature treated coke for the understanding of their carbon molecular structures, *Carbon* 125 (2017) 146–155.
- [3] J. Takashiro, Y. Kudo, S. Kaneko, K. Takai, T. Ishii, T. Kyotani, T. Enoki, M. Kiguchi, Heat treatment effect on the electronic and magnetic structures of nanographene sheets investigated through electron spectroscopy and conductance measurements, *Phys. Chem. Chem. Phys.* 16 (2014) 7280–7289.
- [4] S. Fujii, T. Enoki, Clar's aromatic sextet and pi-electron distribution in nanographene, *Angew. Chem. Int. Ed.* 51 (2012) 7236–7241.
- [5] M. Fujita, K. Wakabayashi, K. Nakada, K. Kusakabe, Peculiar localized state at zigzag graphite edge, *J. Phys. Soc. Jpn.* 65 (1996) 1920–1923.
- [6] M. Acik, G. Lee, C. Mattevi, M. Chhowalla, K. Cho, Y.J. Chabal, Unusual infrared-absorption mechanism in thermally reduced graphene oxide, *Nat. Mater.* 9 (2010) 840–845.
- [7] G. Barco, A. Maranzana, G. Ghigo, M. Causa, G. Tonachini, The oxidized soot surface: theoretical study of desorption mechanisms involving oxygenated functionalities and comparison with temperature programmed desorption experiments, *J. Chem. Phys.* 125 (2006) 194706.
- [8] G.K. Dathar, Y.T. Tsai, K. Gierszal, Y. Xu, C. Liang, A.J. Rondinone, S.H. Overbury, V. Schwartz, Identifying active functionalities on few-layered graphene catalysts for oxidative dehydrogenation of isobutane, *ChemSusChem* 7 (2014) 483–491.
- [9] F. Herold, J. Gläsel, B.J.M. Etzold, M. Rønning, Can Temperature-Programmed Techniques Provide the Gold Standard for Carbon Surface Characterization? *Chem. Mater.* 34 (2022) 8490–8516.
- [10] J.L. Figueiredo, M.F.R. Pereira, M.M.A. Freitas, J.J.M. Orfao, Modification of the surface chemistry of activated carbons, *Carbon* 37 (1999) 1379–1389.
- [11] The Carbon Society of Japan, *新・炭素材料入門* [title in Japanese], REALIZE Science & Engineering, 1996 [in Japanese].
- [12] S. Nagaishi, S. Iwamura, T. Ishii, S.R. Mukai, Clarification of the Effects of Oxygen Containing Functional Groups on the Pore Filling Behavior of Discharge Deposits in Lithium—Air Battery Cathodes Using Surface-Modified Carbon Gels, *J. Phys. Chem. C* 127 (2023) 2246–2257.
- [13] H. Ishitobi, S. Yamamoto, T. Ishii, K. Oba, H. Doki, R. Obata, A. Miyashita, H. Okazaki, N. Nakagawa, Activity Enhancement of a Carbon Electrode Material for Vanadium Redox Flow Battery by Electron-Beam Irradiation, *J. Chem. Eng. Japan* 54 (2021) 219–225.
- [14] T. Ishii, A. Horiuchi, J. Ozaki, An Ion-Sensitive Field Effect Transistor Using Metal-Coordinated Zeolite-Templated Carbons as a Three-Dimensional Graphene Nanoribbon Network, *Front. Mater.* 6 (2019) 129.
- [15] A. Gabe, A. Takatsuki, M. Hiratani, M. Kaneeda, Y. Kurihara, T. Aoki, H. Mashima, T. Ishii, J.-i. Ozaki, H. Nishihara, T. Kyotani, In-Depth Analysis of Key Factors Affecting the Catalysis of Oxidized Carbon Blacks for Cellulose Hydrolysis, *ACS Catal.* 12 (2022) 892–905.
- [16] H. Kim, Y. Lee, D. Lee, G. Park, Y. Yoo, Fabrication of the carbon paper by wet-laying of ozone-treated carbon fibers with hydrophilic functional

- groups, *Carbon* 60 (2013) 429–436.
- [17] K. Jitapunkul, P. Inthasuan, P. Sakulaue, H. Takano, T. Ishii, K. Nueangnoraj, Development of cigarette filter with biomass-based activated carbon for naphthalene removal from mainstream smoke, *Carbon Reports* 1 (2022) 153–161.
- [18] Y. Otake, R.G. Jenkins, Characterization of Oxygen-Containing Surface Complexes Created on a Microporous Carbon by Air and Nitric-Acid Treatment, *Carbon* 31 (1993) 109–121.
- [19] P. Vinke, M. Vandereijk, M. Verbree, A.F. Voskamp, H. Vanbekkum, Modification of the Surfaces of a Gas-Activated Carbon and a Chemically Activated Carbon with Nitric-Acid, Hypochlorite, and Ammonia, *Carbon* 32 (1994) 675–686.
- [20] Q. Zhuang, T. Kyotani, A. Tomita, DRIFT and TK/TPD Analyses of Surface Oxygen Complexes Formed during Carbon Gasification, *Energy Fuels* 8 (1994) 714–718.
- [21] C. Ishizaki, I. Marti, Surface Oxide Structures on a Commercial Activated Carbon, *Carbon* 19 (1981) 409–412.
- [22] P.E. Fanning, M.A. Vannice, A Drifts Study of the Formation of Surface Groups on Carbon by Oxidation, *Carbon* 31 (1993) 721–730.
- [23] S.H. Park, S. McClain, Z.R. Tian, S.L. Suib, C. Karwacki, Surface and bulk measurements of metals deposited on activated carbon, *Chem. Mater.* 9 (1997) 176–183.
- [24] S. Biniak, G. Szymanski, J. Siedlewski, A. Swiatkowski, The characterization of activated carbons with oxygen and nitrogen surface groups, *Carbon* 35 (1997) 1799–1810.
- [25] J.S. Noh, J.A. Schwarz, Effect of Hno<sub>3</sub> Treatment on the Surface-Acidity of Activated Carbons, *Carbon* 28 (1990) 675–682.
- [26] Z. Zhang, D.W. Flaherty, Modified potentiometric titration method to distinguish and quantify oxygenated functional groups on carbon materials by pKa and chemical reactivity, *Carbon* 166 (2020) 436–445.
- [27] S. Kashiwara, S. Otani, H. Orikasa, Y. Hoshikawa, J. Ozaki, T. Kyotani, A quantitative analysis of a trace amount of hydrogen in high temperature heat-treated carbons, *Carbon* 50 (2012) 3310–3314.
- [28] R.T. Meyer, A.W. Lynch, J.M. Freese, M.C. Smith, R.J. Imprescia, Residual Hydrocarbon and Hydrogen Contents of Carbons and Graphites, *Carbon* 11 (1973) 258–260.
- [29] G. Tremblay, F.J. Vastola, P.L. Walker Jr., Thermal Desorption Analysis of Oxygen-Surface Complexes on Carbon, *Carbon* 16 (1978) 35–39.
- [30] I. Gniot, P. Kirszenstejn, M. Kozłowski, Oxidative dehydrogenation of isobutane using modified activated carbons as catalysts, *Appl. Catal. A* 362 (2009) 67–74.
- [31] C. Sentorun-Shalaby, X.H. Ma, C.S. Song, Preparation of High-Performance Adsorbent from Coal for Adsorptive Denitrogenation of Liquid Hydrocarbon Streams, *Energy Fuels* 27 (2013) 1337–1346.
- [32] M.J. Bleda-Martínez, D. Lozano-Castelló, E. Morallón, D. Cazorla-Amorós, A. Linares-Solano, Chemical and electrochemical characterization of porous carbon materials, *Carbon* 44 (2006) 2642–2651.
- [33] R. Berenguer, J.P. Marco-Lozar, C. Quijada, D. Cazorla-Amorós, E. Morallón, A comparison between oxidation of activated carbon by electrochemical and chemical treatments, *Carbon* 50 (2012) 1123–1134.
- [34] A. Dandekar, R.T.K. Baker, M.A. Vannice, Characterization of activated carbon, graphitized carbon fibers and synthetic diamond powder using TPD and drifts, *Carbon* 36 (1998) 1821–1831.
- [35] J.P. Boudou, M. Chehimi, E. Broniek, T. Siemieniowska, J. Bimer, Adsorption of H<sub>2</sub>S or SO<sub>2</sub> on an activated carbon cloth modified by ammonia treatment, *Carbon* 41 (2003) 1999–2007.
- [36] J.P. Boudou, P. Parent, F. Suarez-Garcia, S. Villar-Rodil, A. Martinez-Alonso, J.M.D. Tascon, Nitrogen in aramid-based activated carbon fibers by TPD, XPS and XANES, *Carbon* 44 (2006) 2452–2462.
- [37] Y. Hoshikawa, B.G. An, S. Kashiwara, T. Ishii, M. Ando, S. Fujisawa, K. Hayakawa, S. Hamatani, H. Yamada, T. Kyotani, Analysis of the interaction between rubber polymer and carbon black surfaces by efficient removal of physisorbed polymer from carbon-rubber composites, *Carbon* 99 (2016) 148–156.
- [38] R.S. Ribeiro, A.M.T. Silva, L.M. Pastrana-Martínez, J.L. Figueiredo, J.L. Faria, H.T. Gomes, Graphene-based materials for the catalytic wet peroxide oxidation of highly concentrated 4-nitrophenol solutions, *Catal. Today* 249 (2015) 204–212.
- [39] J.M. Calo, D. Cazorla-Amorós, A. Linares-Solano, M.C. Román-Martínez, C.S.-M. De Lecea, The effects of hydrogen on thermal desorption of oxygen surface complexes, *Carbon* 35 (1997) 543–554.
- [40] L.H. Zhang, J.M. Calo, Thermal desorption methods for porosity characterization of carbons and chars, *Colloids Surf. A Physicochem. Eng. Asp.* 187–188 (2001) 207–218.
- [41] S. Morales-Torres, T.L. Silva, L.M. Pastrana-Martínez, A.T. Brandao, J.L. Figueiredo, A.M. Silva, Modification of the surface chemistry of single- and multi-walled carbon nanotubes by HNO<sub>3</sub> and H<sub>2</sub>SO<sub>4</sub> hydrothermal oxidation for application in direct contact membrane distillation, *Phys. Chem. Chem. Phys.* 16 (2014) 12237–12250.
- [42] A. Pigamo, M. Besson, B. Blanc, P. Gallezot, A. Blackburn, O. Kozynchenko, S. Tennison, E. Crezee, F. Kapteijn, Effect of oxygen functional groups on synthetic carbons on liquid phase oxidation of cyclohexanone, *Carbon* 40 (2002) 1267–1278.
- [43] A.G. Gonçalves, J.L. Figueiredo, J.J.M. Orfao, M.F.R. Pereira, Influence of the surface chemistry of multi-walled carbon nanotubes on their activity as ozonation catalysts, *Carbon* 48 (2010) 4369–4381.
- [44] J. Zhou, Z. Sui, J. Zhu, P. Li, D. Chen, Y. Dai, W. Yuan, Characterization of surface oxygen complexes on carbon nanofibers by TPD, XPS and FT-IR, *Carbon* 45 (2007) 785–796.
- [45] F. Coloma, A. Sepulvedaescrignano, J.L.G. Fierro, F. Rodriguezreinoso, Preparation of Platinum Supported on Pregraphitized Carbon-Blacks, *Langmuir* 10 (1994) 750–755.
- [46] P. Novák, J. Ufheil, H. Buqa, F. Krumeich, M.E. Spahr, D. Goers, H. Wilhelm, J. Dentzer, R. Gadiou, C. Vix-Guterl, The importance of the active surface area of graphite materials in the first lithium intercalation, *J. Power Sources* 174 (2007) 1082–1085.
- [47] S.H. Ng, C. Vix-Guterl, P. Bernardo, N. Tran, J. Ufheil, H. Buqa, J. Dentzer, R. Gadiou, M.E. Spahr, D. Goers, P. Novak, Correlations between surface properties of graphite and the first cycle specific charge loss in lithium-ion batteries, *Carbon* 47 (2009) 705–712.
- [48] T. Ishii, S. Kashiwara, Y. Hoshikawa, J. Ozaki, N. Kannari, K. Takai, T. Enoki, T. Kyotani, A quantitative analysis of carbon edge sites and an estimation of graphene sheet size in high-temperature treated, non-porous carbons, *Carbon* 80 (2014) 135–145.
- [49] T. Ishii, T. Kyotani, Temperature Programmed Desorption, in: M. Inagaki, F. Kang (Eds.), *Materials Science and Engineering of Carbon*, Butterworth-Heinemann, United Kingdom, 2016, pp. 287–305.
- [50] U. Zielke, K.J. Huttinger, W.P. Hoffman, Surface-oxidized carbon fibers. 1. Surface structure and chemistry, *Carbon* 34 (1996) 983–998.
- [51] G. de la Puente, J.J. Pis, J.A. Menéndez, P. Grange, Thermal stability of oxygenated functions in activated carbons, *J. Anal. Appl. Pyrolysis* 43 (1997) 125–138.
- [52] D.M. Nevskaja, A. Santianes, V. Munoz, A. Guerrero-Ruiz, Interaction of aqueous solutions of phenol with commercial activated carbons: an adsorption and kinetic study, *Carbon* 37 (1999) 1065–1074.
- [53] C. Moreno-Castilla, M.A. Ferro-García, J.P. Joly, I. Bautis-Tatoledo, F. Carrasco-Marin, J. Rivera-Utrilla, Activated Carbon Surface Modifications by Nitric-Acid, Hydrogen-Peroxide, and Ammonium Peroxydisul-



- fate Treatments, *Langmuir* 11 (1995) 4386–4392.
- [54] B. Marchon, J. Carrazza, H. Heinemann, G.A. Somorjai, TPD and XPS studies of O<sub>2</sub>, CO<sub>2</sub>, and H<sub>2</sub>O adsorption on clean polycrystalline graphite, *Carbon* 26 (1988) 507–514.
- [55] C. Moreno-Castilla, F. Carrasco-Marín, F.J. Maldonado-Hódar, J. Rivera-Utrilla, Effects of non-oxidant and oxidant acid treatments on the surface properties of an activated carbon with very low ash content, *Carbon* 36 (1998) 145–151.
- [56] N. Li, X. Ma, Q. Zha, K. Kim, Y. Chen, C. Song, Maximizing the number of oxygen-containing functional groups on activated carbon by using ammonium persulfate and improving the temperature-programmed desorption characterization of carbon surface chemistry, *Carbon* 49 (2011) 5002–5013.
- [57] B. Marchon, W.T. Tysoe, J. Carrazza, H. Heinemann, G.A. Somorjai, Reactive and Kinetic-Properties of Carbon-Monoxide and Carbon-Dioxide on a Graphite Surface, *J. Phys. Chem.* 92 (1988) 5744–5749.
- [58] S. Kundu, Y. Wang, W. Xia, M. Muhler, Thermal Stability and Reducibility of Oxygen-Containing Functional Groups on Multiwalled Carbon Nanotube Surfaces: A Quantitative High-Resolution XPS and TPD/TPR Study, *J. Phys. Chem. C* 112 (2008) 16869–16878.
- [59] S. Kundu, W. Xia, W. Busser, M. Becker, D.A. Schmidt, M. Havenith, M. Muhler, The formation of nitrogen-containing functional groups on carbon nanotube surfaces: a quantitative XPS and TPD study, *Phys. Chem. Chem. Phys.* 12 (2010) 4351–4359.
- [60] J.J. Ternero-Hidalgo, J.M. Rosas, J. Palomo, M.J. Valero-Romero, J. Rodríguez-Mirasol, T. Cordero, Functionalization of activated carbons by HNO<sub>3</sub> treatment: Influence of phosphorus surface groups, *Carbon* 101 (2016) 409–419.
- [61] M.J. Valero-Romero, F.J. García-Mateos, J. Rodríguez-Mirasol, T. Cordero, Role of surface phosphorus complexes on the oxidation of porous carbons, *Fuel Process. Technol.* 157 (2017) 116–126.
- [62] T. Ishii, Accurate Analysis of Edge Planes in High-Temperature Treated Carbons for the Understanding of Their Structures and Performances, Tohoku University, 2014.
- [63] T. Ishii, J. Ozaki, Understanding the chemical structure of carbon edge sites by using deuterium-labeled temperature-programmed desorption technique, *Carbon* 161 (2020) 343–349.
- [64] Y. Hoshikawa, R. Kawaguchi, K. Nomura, H. Akahane, T. Ishii, M. Ando, N. Hoshino, T. Akutagawa, H. Yamada, T. Kyotani, Quantitative analysis of the formation mechanism of tightly bound rubber by using carbon-coated alumina nanoparticles as a model filler, *Carbon* 173 (2021) 870–879.
- [65] R. Tang, K. Taguchi, H. Nishihara, T. Ishii, E. Morallon, D. Cazorla-Amoros, T. Asada, N. Kobayashi, Y. Muramatsu, T. Kyotani, Insight into the origin of carbon corrosion in positive electrodes of supercapacitors, *J. Mater. Chem. A Mater. Energy Sustain.* 7 (2019) 7480–7488.
- [66] T. Kyotani, J. Ozaki, T. Ishii, What can we learn by analyzing the edge sites of carbon materials? *Carbon Reports* 1 (2022) 188–205.
- [67] T. Ishii, J. Ozaki, Estimation of the spatial distribution of carbon edge sites in a carbon structure using H<sub>2</sub> desorption kinetics in temperature programmed desorption, *Carbon* 196 (2022) 1054–1062.
- [68] D.A. King, Thermal desorption from metal surfaces: A review, *Surf. Sci.* 47 (1975) 384–402.
- [69] H. Aso, K. Matsuoka, A. Sharma, A. Tomita, Evaluation of size of graphene sheet in anthracite by a temperature-programmed oxidation method, *Energy Fuels* 18 (2004) 1309–1314.
- [70] H. Aso, K. Matsuoka, A. Sharma, A. Tomita, Structural analysis of PVC and PFA carbons prepared at 500–1000 degrees C based on elemental composition, XRD, and HRTEM, *Carbon* 42 (2004) 2963–2973.
- [71] A. Rawal, S.H. Che Man, V. Agarwal, Y. Yao, S.C. Thickett, P.B. Zetterlund, Structural Complexity of Graphene Oxide: The Kirigami Model, *ACS Appl. Mater. Interfaces* 13 (2021) 18255–18263.